The Journal of Chemical Physics

Theoretical inspection of the spin-crossover $[Fe(tzpy)_2(NCS)_2]$ complex on Au(100) surface

Cite as: J. Chem. Phys. **154**, 034701 (2021); https://doi.org/10.1063/5.0036612
Submitted: 09 November 2020 • Accepted: 24 December 2020 • Published Online: 15 January 2021

Carlos M. Palomino, Rocío Sánchez-de-Armas and Carmen J. Calzado

The Journal of Chemical Physics ARTICLE scitation.org/journal/jcp

Theoretical inspection of the spin-crossover $[Fe(tzpy)_2(NCS)_2]$ complex on Au(100) surface

Cite as: J. Chem. Phys. 154, 034701 (2021); doi: 10.1063/5.0036612
Submitted: 9 November 2020 • Accepted: 24 December 2020 •
Published Online: 15 January 2021

Carlos M. Palomino, Rocío Sánchez-de-Armas, and Carmen J. Calzado[a)]

AFFILIATIONS

Departamento de Química Física, c/Profesor García González, s/n 41012 Sevilla, Spain

Note: This paper is part of the JCP Special Collection in Honor of Women in Chemical Physics and Physical Chemistry.
[a)]**Author to whom correspondence should be addressed:** calzado@us.es

ABSTRACT

We explore the deposition of the spin-crossover $[Fe(tzpy)_2(NCS)_2]$ complex on the Au(100) surface by means of density functional theory (DFT) based calculations. Two different routes have been employed: low-cost finite cluster-based calculations, where both the Fe complex and the surface are maintained fixed while the molecule approaches the surface; and periodic DFT plane-wave calculations, where the surface is represented by a four-layer slab and both the molecule and surface are relaxed. Our results show that the bridge adsorption site is preferred over the on-top and fourfold hollow ones for both spin states, although they are energetically close. The LS molecule is stabilized by the surface, and the HS–LS energy difference is enhanced by about 15%–25% once deposited. The different Fe ligand field for LS and HS molecules manifests on the composition and energy of the low-lying bands. Our simulated STM images indicate that it is possible to distinguish the spin state of the deposited molecules by tuning the bias voltage of the STM tip. Finally, it should be noted that the use of a reduced size cluster to simulate the Au(100) surface proves to be a low-cost and reliable strategy, providing results in good agreement with those resulting from state-of-the-art periodic calculations for this system.

INTRODUCTION

Spin crossover (SCO) molecules belong to the family of bistable molecules, capable of reversible switching from a low-spin (LS) electronic state to a high-spin (HS) electronic state, induced by an external stimulus such as temperature, pressure, or light.[1–5] Most of these compounds are pseudo-octahedral Fe (II) complexes (d^6) where the low and high spin states correspond to S = 0 (t_{2g}^6 e_g^0) and S = 2 (t_{2g}^4 e_g^2), respectively. Recently, there has been a remarkable interest in these compounds for their potential applications as molecular switches in signal processing, logic data manipulation, and information storage.[2,3,6–8] To be part of a molecular device, the SCO molecule has to be integrated into a circuit and the spin transition must be preserved once the molecule is deposited on the support.[9–11] The interaction with the support can in fact shift the transition temperatures,[12,13] allow the coexistence of both phases at low temperatures,[14–16] and even suppress the spin transition,[17] blocking the molecule in one of the spin states.

Two main groups of SCO molecules can be distinguished depending on the strength of the interaction – those weakly interacting with the substrate through van der Waals contacts and those with a strong chemical bond with the substrate, mainly through isothiocyanate (–NCS) and isoselenocyanate (–NCSe) ligands, where the terminal S and Se atoms act as surface–molecule anchoring groups. It has been reported that $[Fe(phen)_2(NCS)_2]$, in direct contact with non-magnetic metallic surfaces[18,19] as Cu(100), Au(111), and Cu(111), coexists in both the high- and low-spin states but cannot be switched between them. This has been related to the strong interaction between the complex and the substrate, governed by the chemisorption through the isothiocyanate groups. This strong interaction has also been exploited to build single-molecule STM junctions, such as that made up of the spin-crossover Fe(II) complexes $[Fe(tzpy)_2(NCX)_2]$ (X = S or Se, tzpy = 3-(2-pyridyl)-[1,2,3]triazolo[1,5-*a*]pyridine), on a gold substrate using a magnetic nickel tip,[20,21] or Fe(terpyridine)$_2$ functionalized with a thiol group on the 4 and 4″ positions of the phenyl rings, bridging two gold electrodes.[22]

In this study, we will focus on the $[Fe(tzpy)_2(NCS)_2]$ complex deposited on the Au(100) surface. The adsorption of SCO complexes on this surface has been much less studied than on the other low-index Au-surfaces, but this surface presents the lowest surface energy together with the Au(111) one, and it is the second more abundant in gold nanoparticles.[23] Indeed, the square symmetry of the Au(100) crystalline surface structure offers a unique packing mode for the deposited molecules.

In this $[Fe(tzpy)_2(NCS)_2]$ complex, the Fe(II) metal center lies on an inversion center, and it is coordinated with two tzpy ligands occupying the equatorial positions of a compressed octahedron and two isothiocyanate ligands on axial positions. The experimental data show that it exhibits spin transitions from a low-spin (LS) S = 0 to a high spin (HS) S = 2 state with a critical temperature of $T_{1/2}$ = 108 K for $[Fe(tzpy)_2(NCS)_2]\cdot 2CHCl_3$ and 118 K for $[Fe(tzpy)_2(NCS)_2]\cdot H_2O$.[24] Additionally, two polymorphs without solvent molecules in the lattice have been isolated. Polymorph A exhibits a gradual transition between 180 K and 120 K, while an abrupt transition was observed for polymorph B with transition temperature at 102 K.[25] The enthalpy and entropy changes associated with the spin transition are estimated from calorimetric measurements for $[Fe(tzpy)_2(NCS)_2]\cdot 2CHCl_3$ and $[Fe(tzpy)_2(NCS)_2]\cdot H_2O$ with values of ΔH_{exp} = 3.67 kJ mol^{-1} and 4.08 kJ mol^{-1} and ΔS_{exp} = 34.0 J K^{-1} mol^{-1} and 34.5 J K^{-1} mol^{-1}, respectively.[24] A quantitative light-induced excited spin state trapping (LIESST) effect was observed for $[Fe(tzpy)_2(NCS)_2]\cdot H_2O$[24] and the non-solvated polymorphs.[25]

The aim of this work is to analyze, for the first time, the spin transition process of the $[Fe(tzpy)_2(NCS)_2]$ complex and how it is modified by the deposition on a metal surface. First, geometry optimizations of the free molecule are carried out and the HS–LS energy difference is evaluated with different combinations of exchange-correlation functionals and basis sets. Next, the on-surface spin state switching of this complex is analyzed by two approaches. In the first approach, the Au(100) surface is represented by a finite cluster, and the total energy of the molecule + cluster entity is computed at different distances for on-top and bridge positions. In both cases, the isothiocyanate S atom acts as an anchoring point. In the second step, the deposition is inspected by means of periodic density functional theory (DFT) plane-wave based calculations, where both the surface and molecule are optimized. Our results show that the molecule retains the spin crossover properties once adsorbed, the HS–LS energy is enhanced, and the LS state is favored on the surface with respect to the HS one for all the explored binding positions. All these results are relevant for potential applications as a molecular device. Additionally, the use of a reduced size cluster to simulate the Au(100) surface proves to be a low-cost strategy, providing results in good agreement with those resulting from state-of-the-art periodic calculations. Finally, the STM images have been simulated for both spin states, and the results indicate that it is possible to distinguish between both states using the STM bias voltage as a testing probe.

DESCRIPTION OF THE SYSTEM AND COMPUTATIONAL DETAILS

The main available geometrical parameters for the low- and room temperature structures of this complex are reported in Table I. It should be noted that the inclusion or exclusion of the solvent in the lattice of the SCO complex introduces slight changes in the structure, which induce significant differences in the magnetic properties, as the transition temperatures.[25,26] We use as reference the $[Fe(tzpy)_2(NCS)_2]\cdot 2CHCl_3$ crystal for which the x-ray data are available for the room temperature structure and estimates of the transition entropy and enthalpy have been reported.[24] In the FeN_6 core, the axial positions belong to the isothiocyanate ligands (N_{thio}), while the equatorial positions are occupied by the N atoms of the pyridine (N_{py}) and triazole (N_{triaz}) groups.

The theoretical study of this $[Fe(tzpy)_2(NCS)_2]$ complex will be carried out using density functional theory (DFT) based approaches, both at molecular and periodic levels with the Gaussian 09 package[27] and VASP code,[28–31] respectively. Although the reference theoretical approach when dealing with SCO Fe(II) complexes[32–37] corresponds to wavefunction based methods such as CASSCF/CASPT2[38] and CASSCF/NEVPT2,[39] they are computationally prohibitive for the study of the deposition on the metallic surface. For this reason, we opt to use the DFT approaches in both scenarios, the isolated molecule and the molecule–surface interaction.

As is well known, DFT methods provide accurate structures and vibrational spectra at a reasonable computational cost, but it can be a challenge to correctly describe the energy difference between the two spin states in the SCO complexes. The main difficulty resides on the rearrangements of the occupied orbitals accompanying the SCO

TABLE I. Main geometrical parameters for the $[Fe(tzpy)_2(NCS)_2]$ complex at low and high temperatures (LT, HT), from X-Ray data, compared to those resulting from TPPSh/def2-SVP calculations for the HS and LS states.

Distance (Å)/angle (deg)	Fe–N_{py}	Fe–N_{triaz}	Fe–N_{thio}	Fe–N_{thio}–C(S)
LT exp poly A[25]	2.021	1.973	1.935	174.98
LS calc	2.016	1.962	1.923	179.98
HT exp poly A[25]	2.217	2.181	2.097	174.46
HT exp poly B[25]	2.193	2.174	2.107	177.53
HT exp $CHCl_3$[24]	2.204	2.211	2.113	170.75
HS calc	2.251	2.251	2.027	168.64

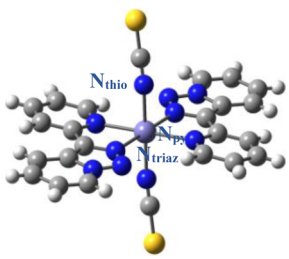

processes, which are exchange-correlation sensitive.[40] Despite the big effort dedicated to obtain a systematic methodology to study the energy of the spin states in different transition metal complexes,[41–45] there is not a definitive XC functional able to compute the relative energy of the LS and HS states, although there exists a certain consensus about the reliability of some functionals. In this study, we first address the evaluation of the HS–LS energy by means of a set of exchange-correlation (XC) functionals and basis sets of different quality. The aim is to establish the best performing XC functional/basis set combination to analyze the spin transition in this Fe(II) complex. The tested XC functionals range from BP86[46,47] [non-hybrid generalized gradient approximation (GGA)], TPSSh[48,49] (hybrid meta-GGA, 10% Fock exchange), B3LYP,[50] and PBE0[51] (20% and 25% Fock, respectively), and the employed basis sets are SDD,[52,53] 6-31G(d,p),[54–57] def2-SVP,[58] TZVP,[59] and the combination QZVP[58] for Fe and TZVP for all non-Fe atoms. The Gaussian 09 package[27] is employed for this set of calculations. Additionally, for comparison, we have carried out the geometry optimization of the free molecule with the ORCA code[60] using both TPSSh and rPBE functionals with the def2-SVP basis set.

To simulate the deposition on the Au(100) surface, we have performed calculations based on the finite size cluster approach and periodic calculations. In both cases, the hexagonal reconstruction of the Au(100) surface is not taken into account, and all the models refer to the native Au(100) bulk surface. First, a three-layer cluster containing 42 Au atoms (21 + 12 + 9) is used. The interlayer separation is 2.07 Å, and the Au–Au distance inside each layer is 2.95 Å. The Fe(II) complex is placed on top of the central Au site, with one of the axial –NCS ligands pointing to the surface, or in a bridge position where the S atom is anchored to two Au atoms. The total energy of the LS and HS solutions has been evaluated at different Au–S distances when the molecule approaches the surface, maintaining fixed its geometry to that of the isolated molecule. The gold atoms are represented with the LANL2DZ basis with the LANL2 relativistic effective core potential.[61] The Gaussian 09 package[27] is employed in all these calculations.

Finally, the adsorption of the $[Fe(tzpy)_2(NCS)_2]$ complex on the Au(100) surface has been studied within periodic DFT with the VASP (Vienna *ab initio* simulation package) code[28–31] using the revised Perdew–Burke–Ernzerhof (rPBE) functional[62] and projector-augmented wave (PAW) potentials.[63,64] The rPBE functional is computationally less expensive than the hybrid ones as TPSSh, and it has been proven to provide a good LS–HS balance (much better than other GGA functionals such as PBE) for well-known SCO complexes containing Fe(II) and Fe(III).[21,22,43] We have tested this functional in a previous study devoted to the deposition of the SCO $[Fe((3,5\text{-}(CH_3)_2Pz)_3BH)_2]$ complex deposited on the Au(111) surface,[65] with excellent agreement with wavefunction based methods such as CASSCF/CASPT2 and CASSCF/NEVPT2 and the available experimental data. Compared with previous DFT+U calculations on the same system,[66] the rPBE functional presents the main advantage of being parameter-free. In fact, LDA+U calculations of the $[Fe((3,5\text{-}(CH_3)_2Pz)_3BH)_2]$ complex showed that the HS–LS energy difference is dramatically sensitive to the U value, much more than usual, providing results in agreement with the experimental data only for a dramatically narrow window of U values between U = 6.5 eV and 6.6 eV.[66] Valence electrons are described using a plane-wave basis set with a cutoff of 500 eV, and the Γ-point of the Brillouin zone is used.[67] The optimized lattice parameters for the Au bulk are a = b = c = 2.97 Å. This calculated value has been used for the (100) surface throughout the present work and maintained fixed during the atomic position relaxation. The Au(100) surface is represented by a slab containing 192 atoms and four layers (23.607 × 17.705 $Å^2$). The atoms of the lowest layer are kept fixed at bulk optimized positions, while the three upper layers as well as the Fe complex have been relaxed. 28 Å of vacuum has been added in the z direction to avoid the interaction between the slabs. The unit cell is big enough to avoid interaction between molecules, as the closest H–H contacts between two molecules along the *a* and *b* axes are found at 8.1 Å and 7.0 Å, respectively. Three starting geometries for geometry optimizations have been used, with one isothiocyanate S atom placed in the top, bridge, or hollow position. Electronic relaxation has been performed until the change in the total energy between two consecutive steps is smaller than 10^{-6} eV, and the ionic relaxation has been performed until the Hellmann–Feynman forces were lower than 0.025 eV/Å. As we are interested in the different magnetic solutions, the NUPDOWN option is used, which forces the difference between the number of electrons in the up and down spin channels, $N_\alpha - N_\beta$, to be equal to 0 (LS) or 4 (HS).

Adsorption energies, E_{ads}, were calculated with respect to the isolated complex on a 23.607 × 17.705 × 35.039 $Å^3$ box as $E_{ads} = E_{adsorbed\_complex} - (E_{slab} + E_{complex})$. Thus, negative adsorption energies represent bound states. The STM simulations with two different bias voltages (−1.5 V and −0.5 V) were carried out using the Tersoff–Hamann approximation.[68] Constant-height STM images were finally visualized in the p4vasp program using density values of 0.00 $e/Å^3$ and 100 $e/Å^3$ as low and high boundaries, respectively. Charge density isosurfaces at 0.05 $e/bohr^3$ are represented with the VESTA code.[69]

RESULTS

Isolated molecule: Choice of the XC functional and basis sets

The Fe(II) complex has been optimized with different basis sets and XC functionals in both spin states and the resulting geometries compared to the available x-ray data for the $[Fe(tzpy)_2(NCS)_2]\cdot 2CHCl_3$ complex at a high temperature.

For all the considered functionals, the calculated bond distances between the Fe center and the axial ligands, $Fe–N_{thio}$, are underestimated, while a slight overestimation of the distances between the metal center and the equatorial ligands $Fe–N_{py}$ and $Fe–N_{triaz}$ is observed. The mean relative errors in Fe–N bond distances are small (1.5%–3.5%) for all the considered functional/basis set combinations (Fig. 1). In fact, the largest deviation comes from the Fe–N–C(S) bond angle (exp 170.7°), underestimated for most of the functionals (mean value for the explored basis sets: 158.7°, 163.6°, and 169.2° for PBE0, TPSSh, and BP86, respectively) and slightly overestimated for B3LYP (173.4°). The BP86 functional results to be less sensitive to the basis set quality. In fact, it is common to optimize the models employed in benchmark studies[42,43] at the BP86/def2-SVP basis level.

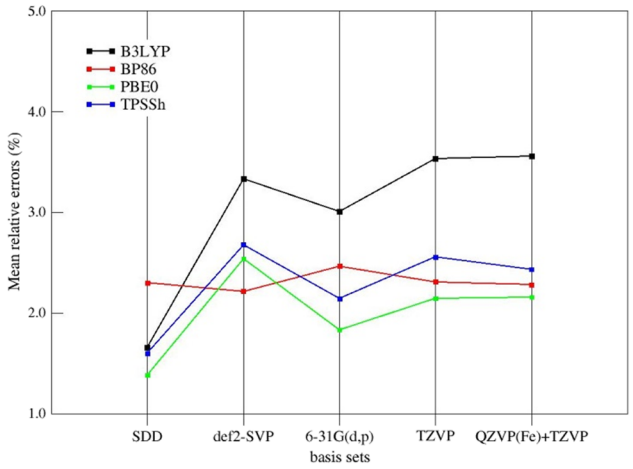

FIG. 1. Mean relative error (%) for Fe–N bond distances for the different XC functional/basis set explored.

Once optimized, the energy difference between the HS and LS state is evaluated for each functional/basis pair (Table II) and compared to the experimental enthalpy change associated with the spin transition, estimated from calorimetric measurements {ΔH_{exp} = 3.67 kJ mol^{-1} and 4.08 kJ mol^{-1} for [Fe(tzpy)$_2$(NCS)$_2$]·2CHCl$_3$ and [Fe(tzpy)$_2$(NCS)$_2$]·H$_2$O, respectively}.[24] PBE0 favors the HS state over the LS one, providing a qualitatively incorrect HS–LS energy difference (negative instead of a positive value) for all the explored basis sets. Similar results are obtained with B3LYP for most of the chosen basis sets. Both TPSSh and BP86 correctly favor the LS state, with a better agreement with the experimental transition enthalpy for TPSSh, in particular for def2-SVP, TZVP, and the combination of QZVP(Fe)+TZVP basis sets. This result is in line with previous benchmark calculations on a set of Fe(II) and Fe(III) SCO complexes.[37,41–43] The geometrical parameters are of similar quality for these three basis sets, but the dimension of the atomic orbital basis is noticeable smaller for def2-SVP. Hence, we decide to use the TPSSh/def2-SVP combination for the study of the deposition of this Fe(II) complex on the Au(100) surface and refine the energetic parameters of the deposited molecules by means of single-point calculations with higher quality basis sets. The bond distances and angles for LS and HS states obtained with this strategy are collected in Table I.

TABLE II. Energy difference (in kJ mol^{-1}) between the optimized geometries of the LS and HS states, HS–LS, with different XC functional/basis pairs. The gray cells correspond to qualitatively correct results, and the white cells correspond to those that predict a wrong sign or a large overestimation of the HS–LS difference.

	XC functional			
Basis sets	B3LYP	BP86	PBE0	TPSSh
SDD	−19.9	68.1	−58.7	−10.1
def2-SVP	−29.1	77.8	−54.0	21.5
6-31G(d, p)	−19.4	89.9	−44.9	35.9
TZVP	20.9	74.9	−56.2	20.9
QZVP(Fe)+TZVP	−30.6	77.2	−56.9	20.3

Additionally, we have also evaluated the performance of the rPBE functional for completeness since the periodic calculations in the section titled Adsorption on Au(100) surface will use this functional. We have carried out the geometry optimization of the free molecule with the ORCA code (rPBE is not available in the Gaussian code) using both TPSSh and rPBE functionals with the def2-SVP basis set. TPSSh is included to check the potential deviations due to the different computational code. The HS–LS energy gaps predicted by these two functionals are consistently similar, with a value of 22 kJ/mol for TPSSh (to be compared with the value of 21.5 kJ/mol when using the Gaussian code, Table I) and 19 kJ/mol in the case of rPBE one, in excellent agreement with the HS–LS gap obtained for the isolated molecule using periodic plane-wave calculations [20.3 kJ mol^{-1}, see the section titled Adsorption on Au(100) surface].

For the free molecule, the difference in the zero-point energy (ZPE) of the LS and HS states is ZPE(HS)–ZPE(LS) = −10.28 kJ mol^{-1}, evaluated from analytic frequency calculations on the optimized geometries at the TPSSh/def2-SVP level. As is well known, the ZPE is more important for the LS state in line with the shorter Fe–N bond distances and then stronger Fe–N bonds. Hence, the zero-point correction favors the HS state in SCO Fe complexes, reducing the HS–LS separation. Thus, the HS–LS separation reduces to 11.2 kJ mol^{-1} for TPSSh/def2-SVP and 10.0 kJ mol^{-1} at the TPSSh/QZVP+TZVP level once the zero-point correction is taken into account, and these values are in reasonable agreement with experimental data.

The molecular orbital diagram for the Fe 3d-like orbitals is shown in Fig. 2 for both spin states. The separation between the barycenter of the t_{2g}-like and e_g-like orbitals is 0.2 hartree for LS, while it reduces to 0.1 hartree in the HS state (Fig. 2). Hence, the ligand field of the Fe center is stronger for the low-temperature structure than the high-temperature one. Consequently, the contribution of the ligands to these orbitals is greater for the LS state than for the HS one, as shown in Fig. 2.

Adsorption on Au(100) surface

The adsorption of the Fe(II) SCO complex on the Au(100) surface has been studied by two different strategies. First, we employ a cluster model for the metal surface and analyze the change in the total energy of the LS and HS states when the molecule approaches the surface, in an on-top position or a bridge position (Fig. 3). In all these calculations, the geometry of the molecule is fixed to the optimized structure of the free molecule on each spin state.

For the on-top position, the LS molecule presents the minimum energy at 2.7 Å above the surface, while the optimal isothiocyanate–surface distance for the HS states is 2.6 Å. The LS solution is more stable than the HS one for all the considered distances (Fig. 4), and the bridge position is favored over the on-top one, as observed for the interaction of the isothiocyanate groups of [Fe(phen)$_2$(NCS)$_2$] with the Cu(001) surface[70] and Co/Cu(111) surface.[71] The bridge sites are found to be also favored for the deposition of alkanethiols on the Au(100)[72] and Au(111)[73,74] substrates.

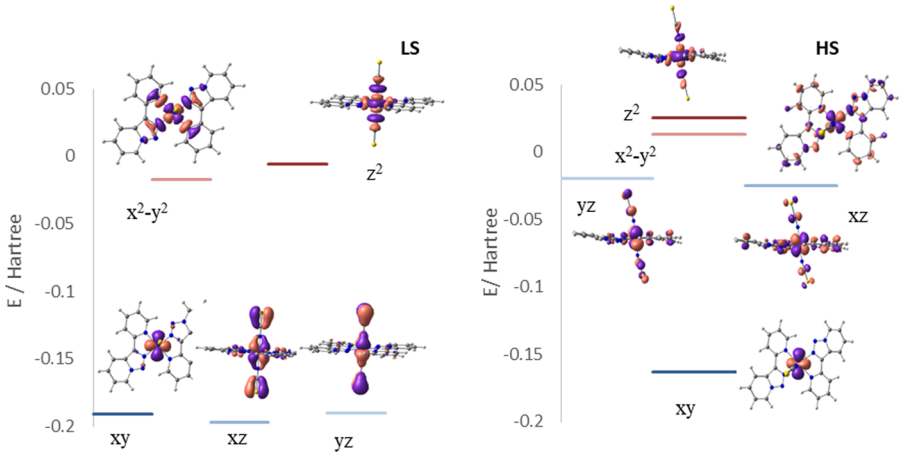

FIG. 2. Molecular orbital diagram for the Fe 3d-like orbitals of the LS(left) and HS(right) states. For the HS state, the 3dxy orbital is doubly occupied, while in the LS state, the $3dx^2 - y^2$ and $3dz^2$ orbitals are unoccupied. The MO energies are obtained at the TPSSh/def2-SVP level.

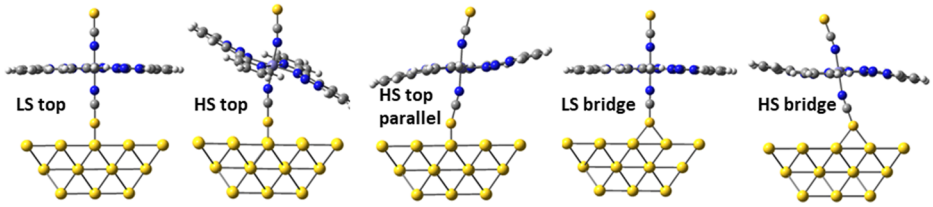

FIG. 3. Geometries adopted for the LS and HS molecules deposited on the Au(100) surface in on-top and bridge positions.

In the bridge position, the molecule is closer to the surface, the optimal molecule–surface distance is 2.3 Å in both states, corresponding to a S–Au distance of 2.73 Å. The separation between the LS and HS curves is almost the same for the two considered Au–S coordination contacts, and in both cases, the transition energy is larger than for the free molecule. Then, the surface induces an enhancement of the relative stability of the LS molecules. In the case of the HS molecule, since the isothiocynate groups are not orthogonal to the tzpy plane, the on-top curve can be estimated with the −NCS axial group perpendicular to the surface as in the LS molecule (HS top in Fig. 3) or by maintaining the tzpy plane parallel to the surface (HS top parallel in Fig. 3). It is interesting that the interaction curves are almost the same (straight cyan and dotted red lines in Fig. 4), regardless of the relative orientation of the molecule with respect to the surface. This indicates that the tzpy ligands are far enough from the surface and do not contribute with any additional interaction with the gold atoms.

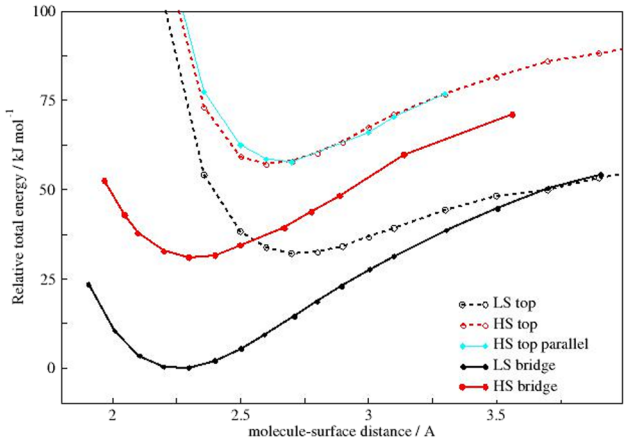

FIG. 4. Total energy (kJ mol^{-1}) of the $[Fe(tzpy)_2(NCS)_2]$ complex, deposited in on-top and bridge sites, in HS and LS states, relative to the LS molecule in the bridge position. All values are at the TPSSh/def2-SVP level.

The adsorption energy can be calculated as $E_{ads} = E_{molec+surf} - (E_{molec} + E_{surf})$. Hence, a negative E_{ads} value means that the molecule-on-surface is stabilized with respect to the free molecule. For the def2-SVP basis, a large basis set superposition error (BSSE) is observed, mostly due to the Fe complex, described with a basis set of poorer quality than the metal cluster. To reduce the BSSE, single-point calculations have been performed for the optimal interaction distance with basis QZVP for Fe and TZVP for the remaining atoms. Similar results are obtained when using the def2-TVZPP basis. The interaction with the surface favors the LS state, and the interaction energy at the optimal S–Au distance is −26.1 kJ mol^{-1} for the LS state and −18.0 kJ mol^{-1} for the HS state for the on-top position, once the BSSE is corrected by the counterpoise approach.[75] For the bridge positions, the interactions energies are stronger with values of −53.6 kJ mol^{-1} for the LS state and −44.0 kJ mol^{-1} for the HS one. This spin-dependent adsorption produces an enhancement of the

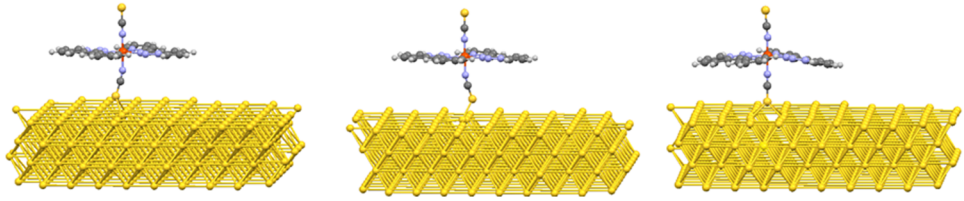

FIG. 5. The deposition of the SCO complex on Au(100) from periodic calculations: on-top (left), bridge (middle), and hollow (right) positions. The LS molecules are represented, similar to the HS ones (Fig. S1).

HS–LS energy difference for the deposited molecule (29.1 kJ mol^{-1} for the on-top position and 30.6 kJ mol^{-1} for the bridge position) with respect to the free molecule (20.3 kJ mol^{-1}) at the same level of calculation.

In the second step, we performed periodic DFT calculations of the molecule deposited on three different positions, on-top, hollow, and bridge (Fig. 5). The geometry of the complex and the upper layers of the gold slab have been fully optimized. The purpose is twofold: first to refine the previous calculations where the geometry of the molecule was fixed to the optimal structure of the isolated molecule for each state and second to test the reliability of the calculations based on finite clusters.

Table III shows the relative energy of the molecule on the three explored positions with respect to the most stable one, the bridge position of the LS molecule. We also report the HS–LS energy for each position as well as the adsorption energies, which reflect the relative stability of the deposited molecule with respect to the free one. The complex adsorbs on the three explored sites (negative E_{ads} in all cases), being the bridge position the preferred one for both spin states, in line with the cluster-based results. The relative stability of the different positions is small (between 1 kJ mol^{-1} and 4 kJ mol^{-1} for on-top with respect to bridge, about 8 kJ mol^{-1} for the difference between hollow and bridge), and then, molecules will be distributed in the different coordination sites on the surface, in particular at room temperature.

For the three considered adsorption sites, the HS–LS energy is enhanced about 15%–25% with respect to the free molecule (29.4 kJ mol^{-1} at the same level of calculation). The same effect has been observed for the $[Fe((3,5\text{-}(CH_3)_2Pz)_3BH)_2]$ complex deposited on the Au(111) surface,[65] $[Fe(phen)_2(NCS)_2]$ on metallic substrates,[70,71] and $[Fe(H_2Bpz_2)_2(bipy)]$ encapsulated in single-walled carbon nanotubes.[76] Hence, the deposition on the surface impacts the relative stability of the HS and LS phases. Although the calculated HS–LS energy is just a rough estimate of the transition enthalpy since effects such as the zero-point correction or collective effects are not included in our evaluations, the fact that the adsorption energy is spin-dependent suggests that the deposition impacts the SCO properties and could modify the transition temperatures as observed for the $[Fe((3,5\text{-}(CH_3)_2Pz)_3BH)_2]$ complex supported on the Au(111) surface[12] and for $[Fe(H_2Bpz_2)_2(bipy)]$ encapsulated in single-walled carbon nanotubes.[76]

The strongest adsorption energies are found for the bridge positions and follow the order bridge > on-top > hollow. Note that, unlike the cluster-based calculations, these adsorption energies also take into account the deformation experienced by the molecule and surface due to the deposition. The adsorption energies are about 50 kJ mol^{-1}, spin-dependent, −59.2 kJ mol^{-1} for LS and −51.4 kJ mol^{-1} for HS for the bridge site, and larger than those calculated for systems where the molecule–substrate deposition is governed by van der Waals interactions, such as $[Fe((3,5\text{-}(CH_3)_2Pz)_3BH)_2]$ on Au(111)[65] and $[Fe(H_2B(pz)_2)_2(bipy)]$ confined in a single-walled carbon nanotube.[76] Our estimates are however four times less than the values reported for the chemisorption of $[Fe(phen)_2(NCS)_2]$ on metallic surfaces.[70] This suggests that

TABLE III. Relative energy of the deposited LS and HS molecules (kJ mol^{-1}), HS–LS energy difference, and adsorption energy in on-top, bridge, and hollow positions on the Au(100) surface from periodic calculations. The HS–LS transition energy for the free molecule is 29.4 kJ mol^{-1} at the same level of calculation.

	Relative energy			Adsorption energy	
Position	LS	HS	HS–LS	LS	HS
On-top	4.4	38.3	33.9	−54.8	−50.4
Bridge	0.00	37.3	37.3	−59.2	−51.4
Hollow	7.9	44.5	36.5	−51.3	−44.2

	LS state S–Au distances (Å)				HS state S–Au distances (Å)			
On-top	2.556				2.673			
Bridge	2.675	2.644			2.723	2.686		
Hollow	2.811	2.848	2.825	2.868	2.884	2.863	2.970	2.989

the on-surface SCO behavior of the $[Fe(tzpy)_2(NCS)_2]$ complex could be different from that reported for the $[Fe(phen)_2(NCS)_2]$ molecule. The adsorption always favors the LS state (with larger E_{ads}), as has been also observed in our cluster-based calculations. The optimal distance to the surface increases with the number of S–Au contacts ($d_{on\text{-}top} < d_{bridge} < d_{hollow}$), in reasonable agreement with the minima in Fig. 4, and they are slightly shorter for the LS than the HS molecules. This is in line with a stronger interaction for the LS molecules, and both can be related to the strength of the Fe ligand field that enhances the metal–ligand hybridization in the LS state. Figure 6 (bottom) shows the density of states of the LS and HS molecules deposited on the Au(100) surface, projected on the Fe atom, isothiocyanate, and tzpy ligands. The most significant difference between both states is the hybridization between the Fe and the ligand states, which is larger for the LS state, in particular for the unoccupied bands. This result is in line with the composition of the Fe 3d-like orbitals discussed above (Fig. 2), where the contribution of the ligands to the eg-like orbitals ($3dx^2 - y^2$ and $3dz^2$) is more important for the LS state than the HS one. In the case of the occupied bands, the main metal–ligand hybridization proceeds through the isothiocyanate groups for the bands close to the Fermi level, as observed for the 3dxz-like and 3dyz-like orbitals in Fig. 2. Comparing with the projected DOS of the free molecule (Fig. 6 top), the main difference comes from the NCS group closest to the surface (NCS1 in Fig. 6), and the states, indistinguishable to those of the NCS2 for the free molecule, strongly differentiate when the molecule is deposited, due to the mixing with the occupied and empty states of the gold surface, in line with the formation of a bond between the terminal S atom and the surface gold atoms. Additionally, the states of the tzpy ligands are slightly shifted to lower energies.

Taking into account the role of the NCS groups in the low-lying occupied bands and the fact that they appear at different energies depending on the spin state, it could be possible to distinguish the adsorbed molecules using a STM tip, as observed for $[Fe((3,5\text{-}(CH_3)_2Pz)_3BH)_2]$ on Au(111).[12] Our simulated STM images (Fig. 7), based on the DOS resulting from the rPBE calculations, indicate that for a negative bias of −0.5 V, the STM image for HS molecules is completely dark, and only the LS molecules are bright. For a bias of −0.5 V, only the states with energy between the Fermi and −0.5 eV can be probed by the STM tip. In the case of the HS molecule, the occupied states in this range are centered on the Fe site as well as on

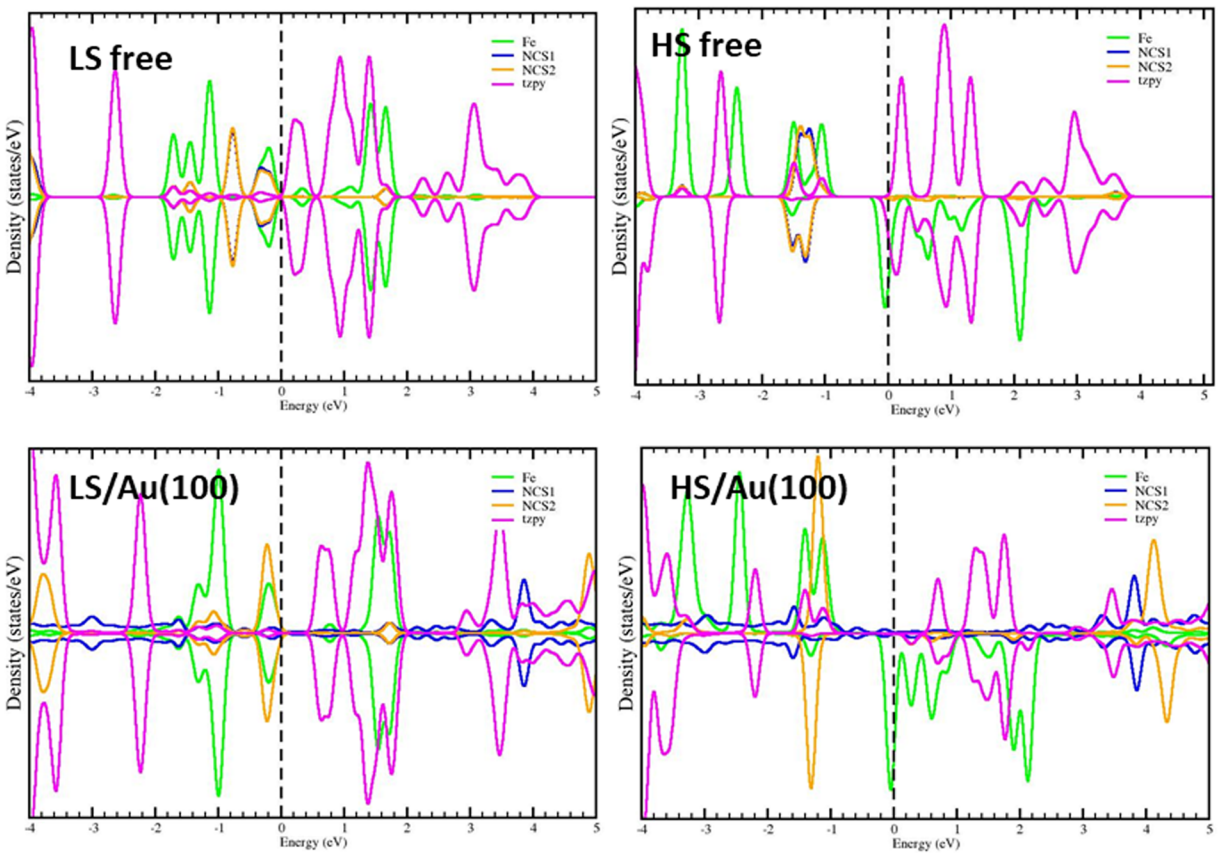

FIG. 6. Projected density of states on Fe, isothiocyanate groups (–NCS1 corresponds to the group closest to the surface), and tzpy ligands for the LS (left) and HS (right) states of the free molecule (top) and deposited in a bridge position (bottom).

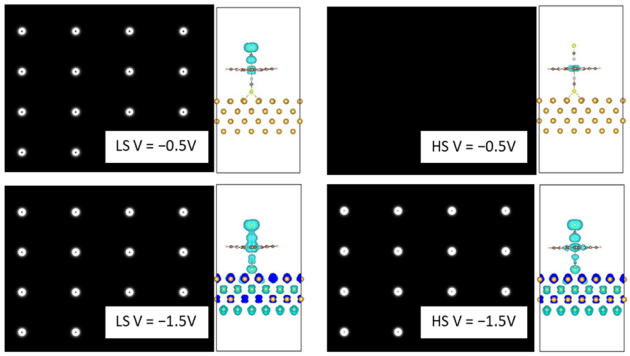

FIG. 7. Constant-height simulated STM images with two different bias voltages (−0.5 V and −1.5 V) for LS (left) and HS (right) states. The images contain 4 × 4 unit cells. On the right-hand side of each STM image, the charge density isosurface at 0.05 e/bohr^3 for the corresponding bias voltage is represented.

the gold surface, both far away from the STM tip. The charge density isosurface at 0.05 e/bohr^3 is represented in Fig. 7 (right-hand side) for each spin state and bias voltage. In the case of the HS molecule with a negative bias of −0.5 V, the density is placed on the Fe 3d orbital, in line with the projected DOS in Fig. 6. However, for the LS molecule, the projected DOS shows a significant contribution of the terminal NCS group, and the states spread enough to be probed by the tip, as the charge density isosurface indicates. Then, at this bias voltage, only the LS molecules can be imaged by STM. For negative bias smaller than −1 V, the spots are similar for both states, in line with the main features of the density of states, and the shape of the charge density isosurface is represented in Fig. 7. Then, it is possible to distinguish the spin state of the deposited molecule using the bias voltage of the STM tip as a probe.

DISCUSSION AND CONCLUDING REMARKS

The on-surface spin state switching of Fe complexes is of relevance for their potential applications in molecular electronics and spintronics, information storage, and sensing. We explore for the first time the interaction of $[Fe(tzpy)_2(NCS)_2]$ with the Au(100) surface by means of DFT calculations. Our calculations indicate that the molecule can adsorb on the three different sites with similar energies, although the bridge coordination is energetically favored, as observed for other Fe SCO complexes on metallic surfaces as well as alkanethiols.

The interaction with the surface is spin-dependent, favors always the LS state, and impacts the SCO properties increasing the HS–LS energy difference. This suggests higher critical temperatures than those reported for the bulk material. It should be noted that the adsorption energies are higher than those estimated for weakly interacting SCO complexes, such as $[Fe((3,5\text{-}(CH_3)_2Pz)_3BH)_2]$ on Au(111), but noticeably smaller than those reported for $Fe(phen)_2(NCS)_2$ on Au(111), Cu(100), and Cu(111), whereas in this case, the complex chemisorbs on the metallic substrate.

In addition to these results, this study brings information about the reliability of the calculations based on finite clusters as models of the gold surface, confronted with the results provided by state-of-the-art periodic DFT evaluations. Our results show a qualitative agreement between both sets of calculations, and the cluster-based calculations correctly predict the optimal adsorption sites and give interaction energies of the same order than those resulting from the periodic calculations, once the basis set superposition errors are corrected. They also agree that the deposition produces an enhancement of the relative stability of the LS state and the spin-dependent hybridization of the 3d-like orbitals due to the different strength of the Fe ligand field on each spin state. The reliability of these cluster-based calculations could be partially ascribed to the fact that the interaction is governed by the terminal isothiocyanate group, and the rest of the molecule has almost no role in the energetics of the deposition. Probably, the scenario would be different for complexes interacting via weak van der Waals contacts where more extended clusters would be necessary to take into account these longer range interactions.

Finally, the simulated STM images show that the spin state of the molecule once deposited can be determined using the bias voltage of the STM tip, and this could be particularly useful at low temperatures, if, as observed for other strongly interacting SCO complexes, the $[Fe(tzpy)_2(NCS)_2]$ molecules coexist in both spin states.

SUPPLEMENTARY MATERIAL

See the supplementary material for the figures for the optimized HS molecules deposited on Au(100) in on-top, bridge, and hollow positions resulting from periodic calculations.

DEDICATION

This paper is dedicated to women scientists of all times who made our work possible today.

ACKNOWLEDGMENTS

The authors acknowledge the financial support by the Ministerio de Ciencia e Innovación-Agencia Estatal de Investigación (Spain) and FEDER funds through Project Grant No. PGC2018-101689-B-I00 (MCI/AEI/FEDER, UE). R.S.-d.-A. thanks VPPI-US for the financial support. The technical support of the Supercomputing Team of the Centro Informático Científico de Andalucía (CICA) and the access to the computational facilities of the "Centro de Servicios de Informática y Redes de Comunicaciones" (CSIRC, Universidad de Granada, Spain) are also acknowledged.

DATA AVAILABILITY

The data that support the findings of this study are available from the corresponding author upon reasonable request.

REFERENCES

[1] P. Gütlich, A. Hauser, and H. Spiering, Angew. Chem., Int. Ed. **33**, 2024–2054 (1994).
[2] A. Bousseksou, G. Molnár, L. Salmon, and W. Nicolazzi, Chem. Soc. Rev. **40**, 3313–3335 (2011).
[3] Z. Liu, S. Ren, and X. Guo, Top. Curr. Chem. **375**, 56 (2017).
[4] O. Kahn, Curr. Opin. Solid State Mater. Sci. **1**, 547–554 (1996).
[5] G. Molnár, S. Rat, L. Salmon, W. Nicolazzi, and A. Bousseksou, Adv. Mater. **30**, 1703862 (2018).
[6] K. Senthil Kumar and M. Ruben, Coord. Chem. Rev. **346**, 176–205 (2017).
[7] A. Cannizzo, C. J. Milne, C. Consani, W. Gawelda, C. Bressler, F. van Mourik, and M. Chergui, Coord. Chem. Rev. **254**, 2677–2686 (2010).
[8] J. A. Real, A. B. Gaspar, and M. C. Muñoz, Dalton Trans. **2005**, 2062–2079.
[9] D. Xiang, X. Wang, C. Jia, T. Lee, and X. Guo, Chem. Rev. **116**, 4318–4440 (2016).
[10] M. Bernien, H. Naggert, L. M. Arruda, L. Kipgen, F. Nickel, J. Miguel, C. F. Hermanns, A. Krüger, D. Krüger, E. Schierle, E. Weschke, F. Tuczek, and W. Kuch, ACS Nano **9**, 8960–8966 (2015).
[11] S. Shi, G. Schmerber, J. Arabski, J.-B. Beaufrand, D. J. Kim, S. Boukari, M. Bowen, N. T. Kemp, N. Viart, G. Rogez, E. Beaurepaire, H. Aubriet, J. Petersen, C. Becker, and D. Ruch, Appl. Phys. Lett. **95**, 043303 (2009).
[12] K. Bairagi, A. Bellec, C. Fourmental, O. Iasco, J. Lagoute, C. Chacon, Y. Girard, S. Rousset, F. Choueikani, E. Otero, P. Ohresser, P. Sainctavit, M.-L. Boillot, T. Mallah, and V. Repain, J. Phys. Chem. C **122**, 727–731 (2018).
[13] V. Davesne, M. Gruber, M. Studniarek, W. H. Doh, S. Zafeiratos, L. Joly, F. Sirotti, M. G. Silly, A. B. Gaspar, J. A. Real, G. Schmerber, M. Bowen, W. Weber, S. Boukari, V. Da Costa, J. Arabski, W. Wulfhekel, and E. Beaurepaire, J. Chem. Phys. **142**, 194702 (2015).
[14] T. Miyamachi, M. Gruber, V. Davesne, M. Bowen, S. Boukari, L. Joly, F. Scheurer, G. Rogez, T. K. Yamada, P. Ohresser, E. Beaurepaire, and W. Wulfhekel, Nat. Commun. **3**, 938 (2012).
[15] H. Naggert, J. Rudnik, L. Kipgen, M. Bernien, F. Nickel, L. M. Arruda, W. Kuch, C. Näther, and F. Tuczek, J. Mater. Chem. C **3**, 7870–7877 (2015).
[16] K. Bairagi, O. Iasco, A. Bellec, A. Kartsev, D. Li, J. Lagoute, C. Chacon, Y. Girard, S. Rousset, F. Miserque, Y. J. Dappe, A. Smogunov, C. Barreteau, M.-L. Boillot, T. Mallah, and V. Repain, Nat. Commun. **7**, 12212 (2016).
[17] A. Pronschinske, Y. Chen, G. F. Lewis, D. A. Shultz, A. Calzolari, M. Buongiorno Nardelli, and D. B. Dougherty, Nano Lett. **13**, 1429–1434 (2013).
[18] M. Gruber, T. Miyamachi, V. Davesne, M. Bowen, S. Boukari, W. Wulfhekel, M. Alouani, and E. Beaurepaire, J. Chem. Phys. **146**, 092312 (2017).
[19] M. Gruber, V. Davesne, M. Bowen, S. Boukari, E. Beaurepaire, W. Wulfhekel, and T. Miyamachi, Phys. Rev. B **89**, 195415 (2014).
[20] A. C. Aragonès, D. Aravena, J. I. Cerdá, Z. Acís-Castillo, H. Li, J. A. Real, F. Sanz, J. Hihath, E. Ruiz, and I. Díez-Pérez, Nano Lett. **16**, 218–226 (2016).
[21] D. Aravena and E. Ruiz, J. Am. Chem. Soc. **134**, 777–779 (2012).
[22] R. Frisenda, G. D. Harzmann, J. A. Celis Gil, J. M. Thijssen, M. Mayor, and H. S. J. van der Zant, Nano Lett. **16**, 4733–4737 (2016).
[23] J. C. Azcárate, G. Corthey, E. Pensa, C. Vericat, M. H. Fonticelli, R. C. Salvarezza, and P. Carro, J. Phys. Chem. Lett. **4**, 3127–3138 (2013).
[24] V. Niel, A. B. Gaspar, M. C. Muñoz, B. Abarca, R. Ballesteros, and J. A. Real, Inorg. Chem. **42**, 4782–4788 (2003).
[25] C.-F. Sheu, K. Chen, S.-M. Chen, Y.-S. Wen, G.-H. Lee, J.-M. Chen, J.-F. Lee, B.-M. Cheng, H.-S. Sheu, N. Yasuda, Y. Ozawa, K. Toriumi, and Y. Wang, Chem. Eur. J. **15**, 2384–2393 (2009).
[26] J. A. Real, A. B. Gaspar, V. Niel, and M. C. Muñoz, Coord. Chem. Rev. **236**, 121–141 (2003).
[27] M. J. Frisch, H. B. Schlegel, G. E. Scuseria, M. A. Robb, J. R. Cheeseman, G. Scalmani, V. Barone, G. A. Petersson, H. Nakatsuji, X. Li, M. Caricato, A. Marenich, J. Bloino, B. G. Janesko, R. Gomperts, B. Mennucci, H. P. Hratchian, J. V. Ortiz, A. F. Izmaylov, J. L. Sonnenberg, D. Williams-Young, F. Ding, F. Lipparini, F. Egidi, J. Goings, B. Peng, A. Petrone, T. Henderson, D. Ranasinghe, V. G. Zakrzewski, J. Gao, N. Rega, G. Zheng, W. Liang, M. Hada, M. Ehara, K. Toyota, R. Fukuda, J. Hasegawa, M. Ishida, T. Nakajima, Y. Honda, O. Kitao, H. Nakai, T. Vreven, K. Throssell, J. A. Montgomery, Jr., J. E. Peralta, F. Ogliaro, M. Bearpark, J. J. Heyd, E. Brothers, K. N. Kudin, V. N. Staroverov, T. Keith, R. Kobayashi, J. Normand, K. Raghavachari, A. Rendell, J. C. Burant, S. S. Iyengar, J. Tomasi, M. Cossi, J. M. Millam, M. Klene, C. Adamo, R. Cammi, J. W. Ochterski, R. L. Martin, K. Morokuma, O. Farkas, J. B. Foresman, and D. J. Fox, "Gaussian 09, Revision B.01" (Gaussian, Inc., Wallingford, CT, 2016).
[28] G. Kresse and J. Furthmüller, Phys. Rev. B **54**, 11169–11186 (1996).
[29] G. Kresse and J. Furthmüller, Comput. Mater. Sci. **6**, 15–50 (1996).
[30] G. Kresse and J. Hafner, Phys. Rev. B **47**, 558–561 (1993).
[31] G. Kresse and J. Hafner, Phys. Rev. B **49**, 14251–14269 (1994).
[32] K. Pierloot and S. Vancoillie, J. Chem. Phys. **128**, 034104 (2008).
[33] B. Ordejón, C. de Graaf, and C. Sousa, J. Am. Chem. Soc. **130**, 13961–13968 (2008).
[34] M. Kepenekian, V. Robert, B. Le Guennic, and C. de Graaf, J. Comput. Chem. **30**, 2327–2333 (2009).
[35] C. Sousa, C. de Graaf, A. Rudavskyi, and R. Broer, J. Phys. Chem. A **121**, 9720–9727 (2017).
[36] N. Suaud, M.-L. Bonnet, C. Boilleau, P. Labèguerie, and N. Guihéry, J. Am. Chem. Soc. **131**, 715–722 (2009).
[37] M. Pápai, G. Vankó, C. de Graaf, and T. Rozgonyi, J. Chem. Theory Comput. **9**, 509–519 (2013).
[38] K. Andersson, P. A. Malmqvist, and B. O. Roos, J. Chem. Phys. **96**, 1218–1226 (1992).
[39] C. Angeli, R. Cimiraglia, S. Evangelisti, T. Leininger, and J.-P. Malrieu, J. Chem. Phys. **114**, 10252–10264 (2001).
[40] K. P. Jensen and J. Cirera, J. Phys. Chem. A **113**, 10033–10039 (2009).
[41] J. Cirera, M. Via-Nadal, and E. Ruiz, Inorg. Chem. **57**, 14097–14105 (2018).
[42] K. P. Kepp, Inorg. Chem. **55**, 2717–2727 (2016).
[43] O. S. Siig and K. P. Kepp, J. Phys. Chem. A **122**, 4208–4217 (2018).
[44] M. Reiher, Inorg. Chem. **41**, 6928–6935 (2002).
[45] S. Ye and F. Neese, Inorg. Chem. **49**, 772–774 (2010).
[46] A. D. Becke, Phys. Rev. A **38**, 3098–3100 (1988).
[47] J. P. Perdew, Phys. Rev. B **33**, 8822–8824 (1986).
[48] J. Tao, J. P. Perdew, V. N. Staroverov, and G. E. Scuseria, Phys. Rev. Lett. **91**, 146401 (2003).
[49] V. N. Staroverov, G. E. Scuseria, J. Tao, and J. P. Perdew, J. Chem. Phys. **119**, 12129–12137 (2003).
[50] A. D. Becke, J. Chem. Phys. **98**, 5648–5652 (1993).
[51] C. Adamo and V. Barone, J. Chem. Phys. **110**, 6158–6170 (1999).
[52] M. Dolg, U. Wedig, H. Stoll, and H. Preuss, J. Chem. Phys. **86**, 866–872 (1987).
[53] T. H. Dunning, Jr., J. Chem. Phys. **53**, 2823–2833 (1970).
[54] R. Ditchfield, W. J. Hehre, and J. A. Pople, J. Chem. Phys. **54**, 724–728 (1971).
[55] V. A. Rassolov, J. A. Pople, M. A. Ratner, and T. L. Windus, J. Chem. Phys. **109**, 1223–1229 (1998).
[56] P. C. Hariharan and J. A. Pople, Theor. Chim. Acta **28**, 213–222 (1973).
[57] W. J. Hehre, R. Ditchfield, and J. A. Pople, J. Chem. Phys. **56**, 2257–2261 (1972).
[58] F. Weigend, Phys. Chem. Chem. Phys. **8**, 1057–1065 (2006).
[59] A. Schäfer, C. Huber, and R. Ahlrichs, J. Chem. Phys. **100**, 5829–5835 (1994).
[60] F. Neese, Wiley Interdiscip. Rev. Comput. Mol. Sci. **2**, 73–78 (2012).
[61] P. J. Hay and W. R. Wadt, J. Chem. Phys. **82**, 299–310 (1985).
[62] B. Hammer, L. B. Hansen, and J. K. Nørskov, Phys. Rev. B **59**, 7413–7421 (1999).
[63] P. E. Blöchl, Phys. Rev. B **50**, 17953–17979 (1994).
[64] G. Kresse and D. Joubert, Phys. Rev. B **59**, 1758–1775 (1999).
[65] N. Montenegro-Pohlhammer, R. Sánchez-de-Armas, and C. J. Calzado, Chem. Eur. J. **27**, 712–723 (2021).
[66] C. Fourmental, S. Mondal, R. Banerjee, A. Bellec, Y. Garreau, A. Coati, C. Chacon, Y. Girard, J. Lagoute, S. Rousset, M. L. Boillot, T. Mallah, C. Enachescu,

C. Barreteau, Y. J. Dappe, A. Smogunov, S. Narasimhan, and V. Repain, J. Phys. Chem. Lett. **10**, 4103–4109 (2019).
[67]H. J. Monkhorst and J. D. Pack, Phys. Rev. B **13**, 5188–5192 (1976).
[68]J. Tersoff and D. R. Hamann, Phys. Rev. B **31**, 805–813 (1985).
[69]K. Momma and F. Izumi, J. Appl. Crystallogr. **44**, 1272–1276 (2011).
[70]S. Gueddida and M. Alouani, Phys. Rev. B **87**, 144413 (2013).
[71]S. Gueddida, M. Gruber, T. Miyamachi, E. Beaurepaire, W. Wulfhekel, and M. Alouani, J. Phys. Chem. Lett. **7**, 900–904 (2016).
[72]D. Grumelli, F. L. Maza, K. Kern, R. C. Salvarezza, and P. Carro, J. Phys. Chem. C **120**, 291–296 (2016).
[73]R. Mazzarello, A. Cossaro, A. Verdini, R. Rousseau, L. Casalis, M. F. Danisman, L. Floreano, S. Scandolo, A. Morgante, and G. Scoles, Phys. Rev. Lett. **98**, 016102 (2007).
[74]A. Cossaro, R. Mazzarello, R. Rousseau, L. Casalis, A. Verdini, A. Kohlmeyer, L. Floreano, S. Scandolo, A. Morgante, M. L. Klein, and G. Scoles, Science **321**, 943–946 (2008).
[75]S. F. Boys and F. Bernardi, Mol. Phys. **19**, 553–566 (1970).
[76]J. Villalva, A. Develioglu, N. Montenegro-Pohlhammer, R. Sanchez-de-Armas, A. Gamonal, E. Rial, L. Ruiz-Gonzalez, J. Sanchez-Costa, C. J. Calzado, E. M. Perez, and E. Burzuri, "Spin-state dependent electrical conductivity in single-walled carbon nanotubes encapsulating spin crossover molecules" (submitted).